

X. MISCELLANEOUS PROBLEMS

A. ELECTRONIC DIFFERENTIAL ANALYZER

Prof. Henry Wallman

Dr. A. B. Macnee

R. Maartmann-Moe

Work on the improvement of computing elements has been continued during the past quarter, and the electronic differential analyzer has been used by members of other groups in the Laboratory to assist them in their investigations. The computing techniques of the electronic differential analyzer have been further applied to the development of a new computing device for the evaluation of Fourier transforms.

1. Computing Elements

Considerable time has been spent on improving the rise time of the magnetic input channel to the crossed-fields multiplier, bringing the rise time down to 10 microseconds, the same as for the electrostatic channel. The requirements on the driving stage in relation to the properties of the magnetic-field coil and the rise time were studied, showing that the power-handling capacity of the driver has to be inversely proportional to the rise time for a given coil damping ratio. The new design uses four 807's in push-pull parallel class AB operation, instead of a single 829B as in the previous design. The present coil uses only 440 turns compared to 6000 previously used. Also, the new coil has been clad with magnetic iron, which reduces the driving requirements and improves the field distribution. Resistance and capacitance parallel damping is used on the coil to control the transient behavior.

R. Maartmann-Moe

2. Differential Equations

Mr. E. E. David has been studying starting transients of microwave oscillators when synchronized by a small c-w signal. In this connection, the nonlinear, variable-coefficient equation

$$\frac{d\theta}{dt} + \frac{K_1 \sin\theta - K_2 e^{-\alpha t}}{1 - e^{-\alpha t}} = 0 \quad , \quad (1)$$

(where K_1 , K_2 , C , and α are constants), has been solved on the electronic differential analyzer with gratifying results. These investigations will be described in a forthcoming Technical Report (No. 100).

(X. MISCELLANEOUS PROBLEMS)

The simultaneous nonlinear equations

$$\frac{dy}{dt} = K_1 y (y_{01} - y - 2x) , \quad (2)$$

$$\frac{dx}{dt} = K_2 x (x_{01} - x - 2y) , \quad (3)$$

(K_1 , K_2 , y_{01} , and x_{01} are constants) have been solved on the electronic differential analyzer by Mr. W. E. Vivian. These equations arise in the study of an oscillating system with two degrees of freedom; the variables x and y are proportional to the power in the two possible modes of oscillation.

Mr. W. L. Hatton has employed the analyzer to study the equation

$$C \frac{de}{dt} + \frac{e}{R} + F(e) = i(t) , \quad (4)$$

where $F(e)$ is the nonlinear characteristic of a germanium-crystal diode. This equation describes the behavior of a parallel RC circuit shunted by a crystal diode.

A. B. Macnee

3. Integral Equations

As a first step in the problem of solving integral equations by electronic means, a calculator capable of solving the following equation has been developed:

$$G(\omega) = \int_0^T f(t) \frac{\cos}{\sin} (\omega t) dt. \quad (5)$$

A block diagram of this calculator is shown in Figure X-1.

The adder, function generator, multiplier, and four integrators are all standard computing elements from the electronic differential analyzer. The three potentiometers P_1 , P_2 and P_3 are driven by a synchronous motor through a gear box at 0.6 rps. Two integrators, the adder, and potentiometers P_1 and P_2 are connected in a loop to solve the differential equation

$$\frac{d^2 x}{dt^2} + \left[\frac{\theta}{360} \right]^2 \omega_o^2 x = 0 , \quad (6)$$

where

$$\omega_o^2 = \frac{1}{R_1 C_1 R_2 C_2} \frac{R_4}{R_3} , \quad (7)$$

θ = potentiometer shaft position in degrees.

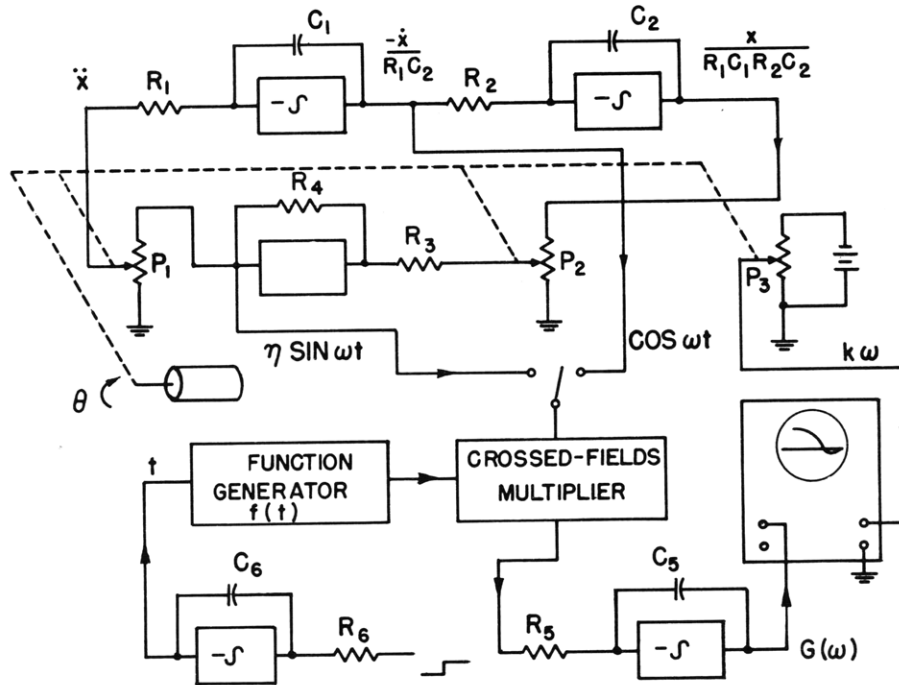


Fig. X-1 Block diagram of Fourier transformer.

Choosing initial conditions $x_0 = 0$, $\dot{x}_0 = 1$, voltages proportional to $\sin \omega t$ and $\cos \omega t$ are available as indicated, with

$$\omega = \omega_0 \left(\frac{\theta}{360} \right) \quad (8)$$

The function to be transformed, $f(t)$, is generated in the function generator and then multiplied by $\cos \omega t$ or $\sin \omega t$ in the crossed-fields multiplier. The output of this multiplier is integrated with respect to time. The value of the integral at $t = T$ is the desired trans-

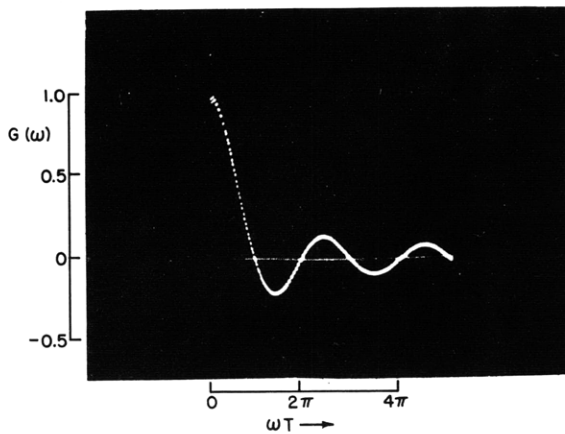


Fig. X-2 Observed cosine transform of $f(t) = C$, $0 < t \leq T$;
 $f(t) = 0$, $t > T$.

(X. MISCELLANEOUS PROBLEMS)

form $G(\omega)$. The individual integrations are performed sixty times per second so that one hundred points are obtained on the $G(\omega)$ curve over the range from zero to ω_0 . The intensity grid of the viewing oscilloscope is gated on for about 10 microseconds at the time $t = T$; thus only the final values of the individual integrations are observed.

Figure X-2 is a photograph of the cosine transform of a square pulse as observed on the output oscilloscope.

A. B. Macnee

B. AN AUTOMATIC IMPEDANCE-FUNCTION ANALYZER

Prof. E. A. Guillemin

R. E. Scott

The general theory of the automatic impedance function analyzer has been given in previous progress reports. During the last quarter, work has continued on the construction of the Mk. 4 machine. Most of the components are now completed and ready for assembly. These components include the following:

1. A 200-line commutator;
2. A 600-probe sampling unit;
3. A 200-point, 3-position, range switch;
4. Sheets of Teledeltos paper with a special coordinate graph printed upon them.

1. The Commutator

The commutator is a mechanical one operating at 600 rpm. It has two banks of 100 contacts and two slip rings. The contacts are brass pins flush-mounted in bakelite. As originally constructed, the commutator was noisy and unreliable. These troubles have been eliminated, however, by the following means:

1. A special shock mount and motor drive which reduce the vibration;
2. New brushes with a resonant frequency of about 2000 cps;
3. Vaseline on the contacts to reduce the friction and to prevent the contacts from scraping off the bakelite and becoming dirty;
4. The use of silver contacts on the brushes.

It has come to our attention that the Mycalex Company of Clifton, New Jersey, have solved a similar problem by using closely spaced contacts, undercut so that the brushes never touch the surface of the background material. This, however, increases the difficulty of manufacture and does not appear to be warranted for the present application.

(X. MISCELLANEOUS PROBLEMS)

2. The Sampling Unit

In order to display the voltage along the imaginary axis upon the face of a cathode-ray tube, a set of probes has been constructed which will sample this voltage at discrete intervals. It was desired to sample not only the voltage (which gives the logarithm of the magnitude of the impedance function) but also the rate of change of the voltage at right angles to the axis. Accordingly, the probes are constructed in two parallel rows 1/10-inch apart, with a spacing of 1/10-inch between the adjacent probes. The probes themselves are copper-plated phonograph needles imbedded in bakelite.

3. The Range Switch

The commutator can handle only one-third of the points at one time. Consequently, only one-third of the range can be viewed at one time on the cathode-ray tube. A range switch has been constructed consisting of banks of 200 banana plugs, which can be placed manually in three different positions.

4. The Sheets of Teledeltos Paper

The size of the sheets of Teledeltos conducting paper has been set at 53 inches by 15.8 inches. This size is a compromise between what would be desirable for accuracy and what can be easily obtained in practice. It allows five decades along the frequency axis, three of which are in the usable region and two of which must be left unused at the ends in order to avoid errors from the finite size of the plane. The decades are 10 inches long, and each of the three centre ones is covered by one of the sets of 200 probes.

The Mk. 4 machine uses a conformal map of the complex frequency plane upon a logarithmic strip. In operating the device, it is convenient to use the original coordinates. Consequently, a map of these coordinates has been prepared and from it the Buck Printing Company of Boston is printing the coordinates upon the Teledeltos paper. Seventy-five sheets are on order at the present time.

C. PROTON-VELOCITY METER

L. D. Smullin

P. Lally

The signal generator and phase-measuring equipment are completed. Further work is awaiting the completion of the Van de Graaff generator installation.

(X. MISCELLANEOUS PROBLEMS)

D. ELECTRONIC-POTENTIAL MAPPING

Dr. S. Goldman
W. F. Santelmann, Jr.
W. E. Vivian

A final report on this project will appear in the July 15, 1949 Quarterly Progress Report. A Technical Report on the project will also be written.

Since the last Progress Report, heart patterns of a number of known pathological cases have been observed, and motion pictures of these patterns have been taken. The patterns of the pathological cases have been clearly different from normal patterns. More pathological patterns are being recorded with the expectation that it will soon be possible to classify the pathological characteristics in the patterns so that they will be useful in diagnosis.

During the past three months, area patterns of the individual lobes of the brain have been observed and photographed. It is found that the occipital and temporal lobes show characteristic traveling-wave patterns. These are being investigated further. A report of this work was presented at the February 19th meeting of the Eastern Association of Electroencephalographers at the Harvard Medical School.

E. THE GENERATION OF MILLIMETER AND INFRARED RADIATION
BY ACCELERATED ELECTRONS

P. D. Coleman

Radiation theory of accelerated electrons was examined in great detail from a quantitative viewpoint by Dr. E. A. Lewis, formerly of this Laboratory, with the object of determining the possibility of generating millimeter waves; one proposal involved the use of a staggered magnetic field to impose small lateral accelerations on a beam of electrons. In the present work, a study of several types of electron trajectories has been made with the objective of seeing if a millimeter or infrared generator based on the radiation from accelerated electrons would be feasible.

One such trajectory of electrons is a small harmonic oscillation imposed on a linear motion as illustrated in Figure X-3. This motion is described by the equations

$$Y = a \sin 2\pi \frac{x}{\lambda_e}, \quad \text{and} \quad x = vt \quad ; \quad (1)$$

hence

$$Y = a \sin \frac{2\pi c}{\lambda_e \beta} t = a \sin \omega_{osc} t \quad . \quad (2)$$

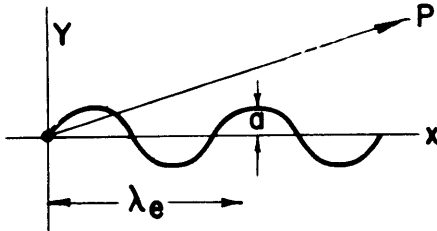


Fig. X-3 Sine-wave path.

To an observer P, whose position vector makes an angle θ with the X-axis, the radiating electron appears as an oscillator of frequency ω_{osc} coming toward him with velocity $v \cos \theta$, so that the frequency of the waves he receives is given by

$$\omega_P = \omega_{osc} (1 - \beta \cos \theta) \quad \text{or} \quad \lambda_P = \frac{\lambda_e}{\beta} (1 - \beta \cos \theta). \quad (3)$$

If, for example, $\cos \theta = 1$, $\beta = 0.98$ (~ 2 Mev), and $\lambda_e = 1$ cm, then $\lambda_P = 0.02$ cm. For $\beta = 0.996$ (~ 5 Mev), $\lambda_P = 0.004$ cm, etc.

The average power radiated by an electron following the above "sine wave" can be shown to be

$$P = 3.59 \left(\frac{a}{\lambda_e} \right)^2 \frac{\beta^4}{(1 - \beta^2)^2} \times 10^{-17} \text{ watts}. \quad (4)$$

For example, $\lambda_e = 2$ cm, $a = 0.1$ cm, $\beta = 0.99$ (~ 3 Mev), the average power P_{av} is 0.56×10^{-12} watts.

One method of deriving the formula given in Eq.(4) is to consider the radiation problem in a frame of reference moving with velocity v along the X-axis, i.e., with the electron. The motion of the electron in this system is a simple harmonic motion about the origin. Calling ω' the frequency of the oscillator in this system ($\omega_{osc} = \omega' \sqrt{1 - \beta^2}$), the power radiated is

$$P = \frac{(qa)^2 \mu_0 \omega'^4}{12\pi c} \text{ watts}. \quad (5)$$

The radiative pattern in this moving system is the familiar doughnut pattern. If this pattern is transformed back into the original laboratory system, it is found that most of the radiation is thrown in the forward

(X. MISCELLANEOUS PROBLEMS)

direction as shown in Figure X-4, the gain along the X-axis over the doughnut pattern being $(1 + \beta)/(1 - \beta)$.

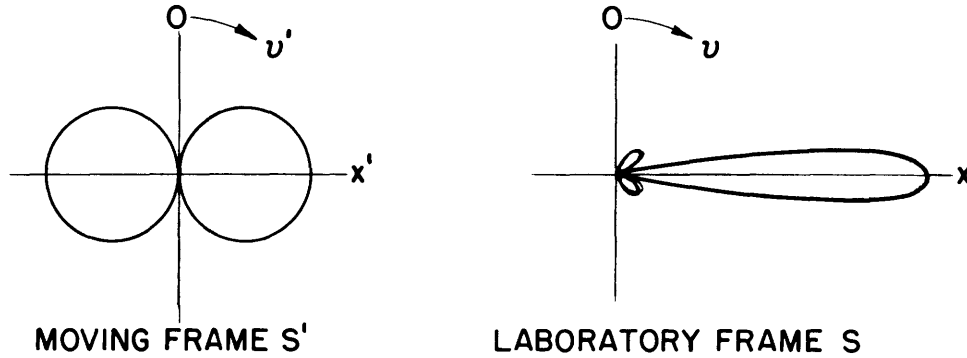


Fig. X-4 Radiative patterns in two frames of reference.

The "sine wave" electron trajectory can be approximated by injecting an electron into a staggered magnetic field, as shown in Figure X-5, where a series of magnets is alternated in polarity. For small amplitude of motion, a , the maximum magnetic field required is

$$B_{\max} \approx \frac{4\pi^2 a}{q\lambda_e^2 c} \beta [T + m_0 c^2] \text{ webers} , \quad (6)$$

where $m_0 c^2 = 0.511 \text{ Mev}$ and T is the kinetic energy of the electrons.

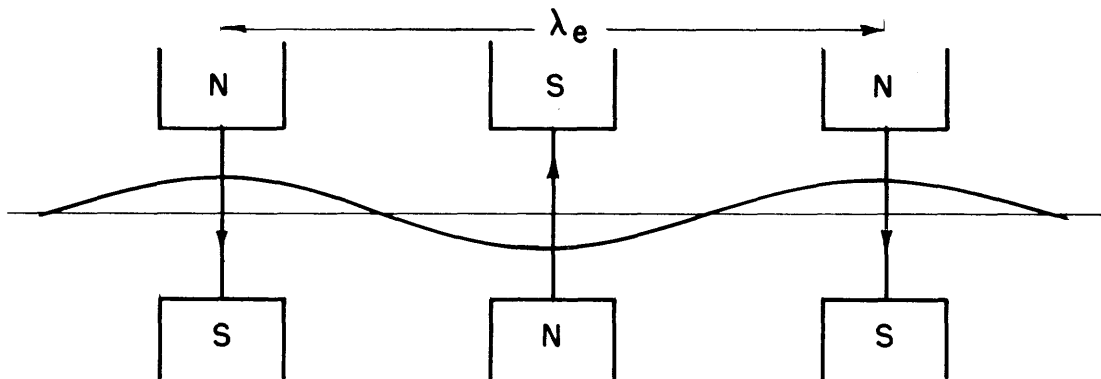


Fig. X-5 Sine-wave magnetic field.

(X. MISCELLANEOUS PROBLEMS)

Using the data $\lambda_e = 4$ cm, $a = 0.1$ cm, and $\beta = 0.99$ (~ 3 Mev), the maximum magnetic field needed is 2,858 gauss.

The principal problem in designing a generator based upon the above physical facts is to get the radiation fields of a large number of electrons to add constructively.

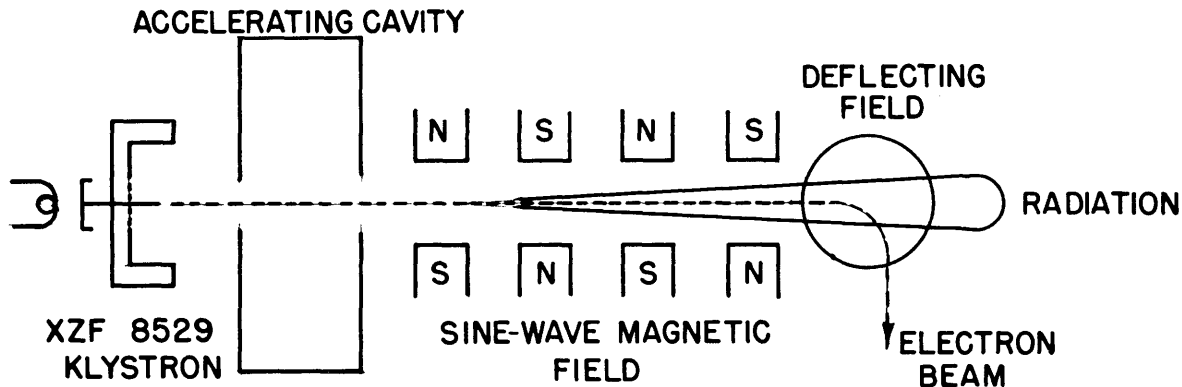


Fig. X-6 Schematic drawing of experimental setup.

One scheme which suggests itself is to inject a bunched electron beam from a klystron source into an accelerating cavity, as illustrated in Figure X-6. The Sperry klystron injects a 0.3-ampere electron beam, space-bunched to the order of millimeters, into a 10 cm cavity accelerator fed by two HK-7 magnetrons, as illustrated in Figure X-7.

The cavity accelerates the electrons to the order of 1 to 1.5 Mev, after which the electrons are injected into the staggered magnetic field. The number of electrons in a bunch coming from the accelerator is of the order of 10^8 so that, if some degree of coherence could be obtained, it is seen from Eq. (4) that appreciable power could be expected (remembering that for

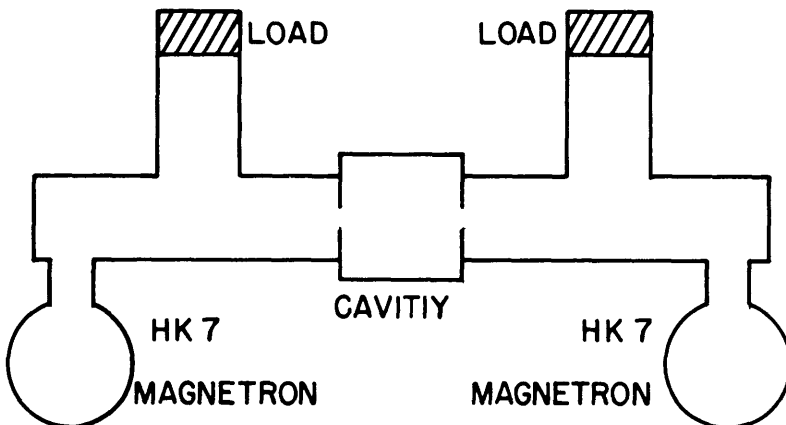


Fig. X-7 Magnetrons feeding cavity accelerator.

(X. MISCELLANEOUS PROBLEMS)

complete coherence the power goes as the square of the number of electrons).

The equipment illustrated in Figures X-6 and X-7 has been built and assembled. However, several technical problems such as prefocusing the electron beam to a small-spot size have delayed the initial test of the apparatus. The magnet spacing in the present equipment has been chosen such that a wavelength of 1.25 cm will be generated for convenience in detecting and measuring the radiation characteristics of the signal.

P. D. Coleman

F. MICROWAVE SECONDARY-EMISSION SWITCH

B. D. Steinberg

It is proposed to use secondary emission in a microwave cavity to devise a high-speed, high-frequency switch. If R is the secondary-emission ratio and n is the number of successive emission, the gain, or ratio of final current to initial current, is R^n . In electrostatic secondary-emission multipliers, n is the number of emitting surfaces. However, if alternating fields are used, such that the electron stream returns m times to each of p surfaces, then $n = m \times p$. In particular, let only two surfaces be used (as in Figure IX-8), with an alternating electric field maintained between them. If the gap distance d , the peak amplitude of the generator voltage V , and the frequency $f = \omega/2\pi$ are so adjusted that an electron leaving one plate at time $t = 0$ with a small or zero initial velocity strikes the opposite plate in $\omega t = \pi$ radians (as the field goes through zero), the secondaries produced by this electron will in turn be accelerated to the first plate, and will strike it approximately π radians later. These electrons will

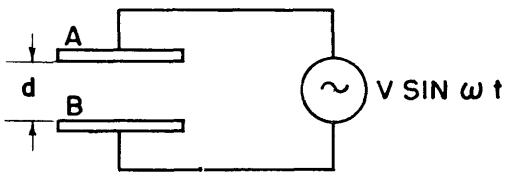


Fig. IX-8 Basic representation of secondary-emission switch.

liberate secondaries which also will be directed by the field to the opposite plate. Hence, if the secondary-emission ratio is greater than unity, the current density in the space between the electrodes will increase.

The conductance of the gap may be defined as the ratio of the current in the gap to the gap voltage. Being linearly related to the current the conductance will increase as the current increases.

Since electrons will successively strike the plates in $\omega t \approx \pi$ radians, the time per interval is π/ω , which decreases as the frequency is raised.

(X. MISCELLANEOUS PROBLEMS)

Thus, at high frequencies only a relatively short time will be required to effect a large change in gap conductance. Hence a tube in which the basic operating principles are similar to that of the illustration of Figure IX-8 may operate as a high-speed high-frequency switch.

Under the conditions shown in Figure X-8, it is hoped to determine the circumstances under which such a secondary-emission tube may be utilized as a high-frequency switch.

The Cavity A 10-cm cavity has been designed and constructed. A simplified cross section is shown in Figure X-9. The gap distance, d , is nominally 0.03 inch and may be varied from 0.015 inch to 0.045 inch by raising and lowering the diaphragm. The opposite faces of the gap consist of beryllium copper, a material whose secondary-emission ratio is approximately 3.5. The remainder of the cavity is copper. The shunt resistance of the cavity is on the order of 500,000 ohms, and the unloaded Q is about 3,000.

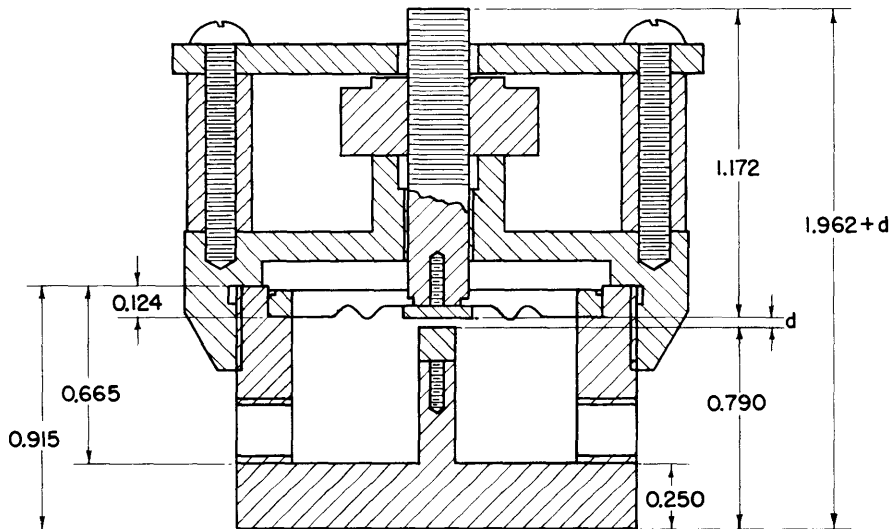
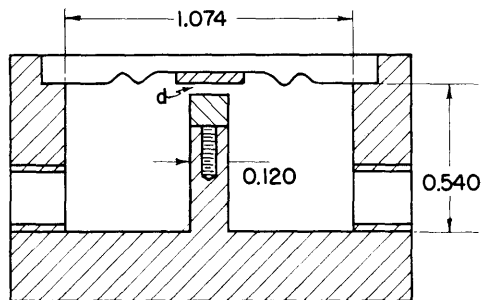


Fig. X-9 Cross section of cavity, complete.



Operation The cavity is interposed between a QK-61 magnetron and a matched load. It is operated on a vacuum pump at a pressure of 5×10^{-5} mm Hg.

(X. MISCELLANEOUS PROBLEMS)

The actual pressure is probably not significant so long as it is below a value at which the mean-free-electron path is several times greater than the gap distance.

Figure X-10 shows the gap voltage, gap current, and ratio of load power to incident power as functions of the incident power; qualitatively, it shows that the ratio of load power to incident power decreases by a factor of five as the incident power is raised from 60 milliwatts to 3 watts. In the absence of an electron current in the gap, the ratio would remain constant. Of further interest is the voltage-current characteristic of the gap, which is determined from standing-wave measurements at the input to the cavity.

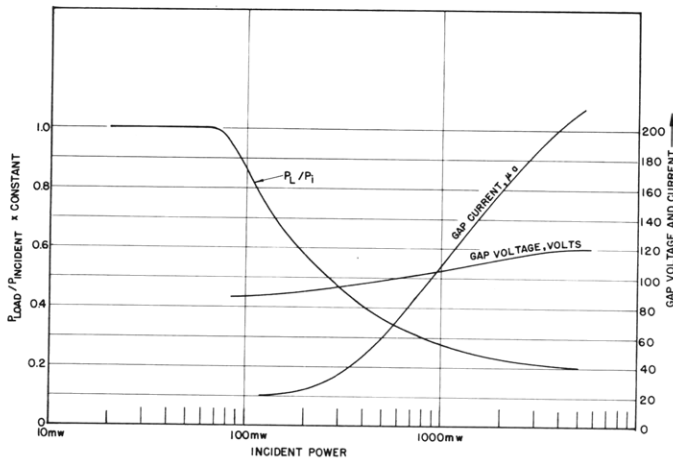


Fig X-10 Operating characteristics of cavity, showing the electron current in the gap, the gap voltage, and the ratio of power transmitted to the load to the power incident upon the cavity as functions of the incident power.

Observations Measurements so far have been qualitative; techniques have yet to be refined before data will be reliable. However, it is fairly certain that the observed behavior of the cavity is due to secondary-electron current in the gap. When conclusive data is obtained at the present power levels, it is proposed to make measurements at higher power by replacing the present power source with a pulsed magnetron. B. D. Steinberg

G. TUBE LABORATORY (Vacuum Systems and Tube Structures)

The Tube Laboratory has been assisting in the design and construction of special vacuum systems for the vacuum spectrograph project of Dr. E. R. Piore. One such apparatus, now nearing completion, is arranged with a modified three-inch brass gate valve (Crane No. 440) and glass stopcocks so that the vacuum chamber may be opened to the atmosphere, changes made in charge or electrical wiring, and evacuation resumed rapidly. The vapor pump is kept running throughout the procedure. The chamber is reduced to forepump pressure through a bypass, and vapor-pump warm-up period is thus eliminated.

The chamber itself has demountable features which will materially shorten

the time necessary to effect changes in setup.

It is hoped that this system will facilitate the testing and study of the behavior of electron guns and other vacuum components for ultimate use in the x-ray spectrograph.

F. Rosebury

H. TUBE LABORATORY (Chemical)

C. S. Pearsall

P. K. Zingesser

1. Brazing To Diamond, Sapphire and Other Nonmetallic Materials

The work on brazing of nonmetallic materials, referred to in the Quarterly Progress Report of October 1948, has been continued, covering the use of several hydrides, special brazing alloys, and various controlled atmospheres. Hydrides of Zirconium, titanium, tantalum, and columbium have yielded good results. Alloys, such as aluminum-silver-zirconium, silver-zirconium, aluminum-zirconium, and silver-titanium, have been successfully used in the brazing of various nonmetallics such as ceramics (steatite, pure refractory oxides), diamond, sapphire, and carbides. Bonds have been successfully prepared in atmospheres of argon with the various hydrides. Both zirconium hydride and zirconium alloys yielded good bonds in an atmosphere of commercial tank nitrogen and helium. Stainless steel and chrome iron have also been brazed in tank nitrogen with zirconium hydride and zirconium alloys. Brazing with titanium was unsuccessful in nitrogen. The successful brazing with zirconium hydride or zirconium alloys in nitrogen atmosphere offers a simple process for bonding ceramics and metals.

2. Properties of Silicon-Germanium Alloys

F. Seitz in 1942, in a discussion of silicon and germanium, suggested that these two elements when alloyed might form semiconductors. It seems likely that germanium-silicon would form a continuous series of solid solutions. The crystal structures are identical, the atomic radii are within a few per cent, and their heats of sublimation and ionization potential are almost identical. Their principal difference lies in their melting points (silicon 1420°C, germanium 958°C). Several alloys of pure germanium and silicon have been prepared by vacuum melting for the investigation of the rectifying properties of these alloys.

An alloy of 50 per cent silicon and 50 per cent germanium by weight gave a remarkably high thermoelectric power -- for example, 900 microvolts per degree C against copper in the range of 25° - 100°C. Some preliminary measurements gave a rectifying ratio of 1:4. Other alloys have been prepared and are being measured.

C. S. Pearsall